Journal of the European Ceramic Society 22 (2002) 2719–2725

www.elsevier.com/locate/jeurceramsoc

Low density biomorphic silicon carbide: microstructure and mechanical properties

F.M. Varela-Feria[a], J. Martínez-Fernández[a], A.R. de Arellano-López[a,*], M. Singh[b]

[a]*Departamento de Física de la Materia Condensada, Universidad de Sevilla, PO Box 1065, 41080 Seville, Spain*
[b]*QSS Group, Inc., NASA Glenn Research Center, Cleveland, OH 44135-3191, USA*

Received 12 December 2001; received in revised form 1 February 2002; accepted 7 March 2002

Abstract

Low density biomorphic SiC ceramics have been fabricated by melt infiltration of pine carbon templates. The resulting porous microstructure is anisotropic and presents a high level of connectivity. Some templates have been partially infiltrated to document the details of the infiltration process. The material has been tested at a constant compression with a strain rate of 2×10^{-5} s^{-1} at high temperatures between 1150 and 1350 °C. The materials showed high compressive strengths relative to the density, with values up to 241 MPa in the axial direction. The compressive strengths relative to those of fully dense SiC are a good extrapolation of previous studies with denser samples, and present qualitative agreement with the model by Gibson and Ashby for plastic collapse of cellular solids. © 2002 Elsevier Science Ltd. All rights reserved.

Keywords: Mechanical properties; Microstructure; Porosity; SiC

1. Introduction

The search for strong, creep-resistant ceramics, has followed several routes. Under well-controlled fabrication procedures, monolithic oxides like mullite, and non-oxides like SiC and Si_3N_4, have proven good candidates for high-temperature applications where strength and constant shape are important.[1] These systems share a complex interlocked grain morphology, and a critical role of grain boundary phases. Limited plasticity in other polycrystals, like alumina or zirconia, has been achieved by means of the addition of whiskers and platelets that impede grain boundary sliding,[2] the most important contributor to macroscopic strain. All these attempts share two important limitations: they are expensive to industrialize and it is difficult to produce net-shaped parts.

Microstructural complexity appears as the key factor in strong ceramics, as it happens in biological structural materials like bones, shells and wood. There have been several efforts to produce artificial microstructures that resemble that of natural materials (continuous-fiber reinforced ceramics,[3] porous ceramics,[4] fibrous ceramics monoliths,[5] etc.). However, natural materials, perfected by time and evolution, also offer unique properties in terms of optimal mechanical response with low density, achieved by a porous and interconnected structure.[6,7]

Biomorphic wood-based SiC has been a matter of interest in recent years.[8–20] The general approach consists of a rapid and controlled mineralization of the wood, with two steps: first the wood is carbonized, and second it undergoes a gas phase infiltration of silicon or a reactive infiltration[21] of molten silicon to produce a SiC material that keeps the wood microstructure. The diversity of wood microstructures offers a large variety of options in terms of materials selections. The two main characteristics that can be selected are the wood density, which results in a particular final SiC density, and the level of anisotropy in mechanical properties in directions parallel (axial) and perpendicular (radial) to the growth direction of the wood. The only necessary condition is that the wood material presents a connected porosity, with a minimum porous size of about 5 μm for efficient infiltration at 1550 °C[22].

* Corresponding author. Tel.: +34-95-455-2894; fax: +34-95-461-2097.
E-mail address: aral@us.es (A.R. de Arellano-López).

0955-2219/02/$ - see front matter © 2002 Elsevier Science Ltd. All rights reserved.
PII: S0955-2219(02)00137-1

In addition to better materials selection, and compared to other SiC fabrication procedures, our method presents the following potential advantages.

- Lower cost: processing temperatures are lower than in other methods, it is not necessary to start out with high-purity powders, and the handling is simpler.
- No additives are used.
- Faster synthesis rate, by using a preform with open cell porosity.
- Complex shapes are easy to obtain: the wood precursor is given a close-to-final shape, and the resultant carbon preform can be machined easily to precise dimensions. In the final infiltration step there is no significant change of volume or change in the parts.

The method used in this study has been successfully applied in the fabrication of SiC from mango tree, American and Spanish oaks, beech and white eucalyptus wood. [11–16,19,20] Several previous publications have covered the outstanding mechanical properties of these SiC materials,[8,11–14,16,19,20,23,24] by detailed compressive strength tests and microstructural characterization.

The final material is composed of SiC and remaining unreacted Si, which amount varies. At high temperatures, it has been found that the mechanical behavior is dominated by the SiC content of the final product, and on the orientation of the experiment relative to direction of the growth of the wood. The correlation between the properties of the woods (at room temperature) is kept in the SiC at high temperatures, but with greatly enhanced strengths. As an example, white eucalyptus wood results in a compressive strength of approximately 50 MPa at room temperature in the direction parallel to that of the growth. At 1150 °C, the compressive strength of the SiC ceramics derived from this wood is larger than 700 MPa, when measured parallel to the growth of the wood. A compressive strength of approximately 200 MPa has been measured at the same temperature, in the direction perpendicular to the growth direction.[19]

Such promising results have been discussed in terms of the cellular solids theory developed by Gibson and Ashby,[4] for plastic collapse of foam and honeycomb structures. This approach assumes that at high temperature the Si imparts negligible resistance compared to the SiC forming a cellular structure. The strength in this theory depends on the relative SiC density of the cellular structure.

Previous studies have covered the range 45–65% of the theoretical density. [11–14,16,19,20] This study focuses in lower density materials, with the objective of extending our previous understanding of the mechanical behavior of these ceramics. The low density of the material is also optimal for getting a first approach to the mechanisms of the infiltration in the fibrous structure, that will also be investigated. Technologically, low-density cellular SiC has important potential applications as high-temperature filters and as catalyst carriers.

2. Experimental details

2.1. Selection of precursor wood and SiC fabrication

The melt infiltration method follows the general flow chart in Fig. 1. The wood is pyrolized in an argon atmosphere at 1000 °C with well-controlled heating and cooling ramps. Then, the liquid silicon infiltration is performed in vacuum. Details of the fabrication process are described in the literature.[12–15]

Previous studies have proven that the melt infiltration method allows good control of the shape and density of the final product by choosing the appropriate wood.[20,22] Typically in all kind of woods, approximately $74 \pm 5\%$ of the starting weight of the natural original material is lost during the pyrolysis, mainly in the form of water vapor and other volatiles. Volume is reduced at the same time by about $60 \pm 5\%$. The SiC density vs. the wood density shows a good linear fit:

$$\rho_{\mathrm{SiC}} = (2.39 \pm 0.01)\rho_{\mathrm{Wood}} \quad R^2 = 0.99 \tag{1}$$

As the theoretical density of SiC, 3.21 g cm^{-3}, for a final relative density SiC in the order of 35%, it is necessary to search woods of densities of about 0.47 g cm^{-3}. Two varieties of the pine, with densities 0.48 ± 0.05 g cm^{-3} (white pine) and 0.53 ± 0.05 g cm^{-3} (Flanders pine), were selected as a precursors. Density measurements here were made geometrically.

The pyrolysis of the woods and the subsequent infiltration of the carbon templates proceeded according to the program in Fig. 1. To achieve complete carbon reaction, the amount of Si added typically exceeded that determined by the stoichiometry. Higher-density carbon templates need 20% excess of Si. This excess increases as density of the carbon templates decreases. In the case of pine-wood carbon templates, previous experience suggests that the amount of Si needs to be a factor of 2 of that determined by stoichiometry. It is expected then that the amount of unreacted Si in the pine-derived SiC is higher than in the denser biomorphic SiC.

Some of the Flanders pine templates were infiltrated with a reduced amount of Si, to allow only partial reaction. The remaining unreacted carbon was burned out by heating in air.

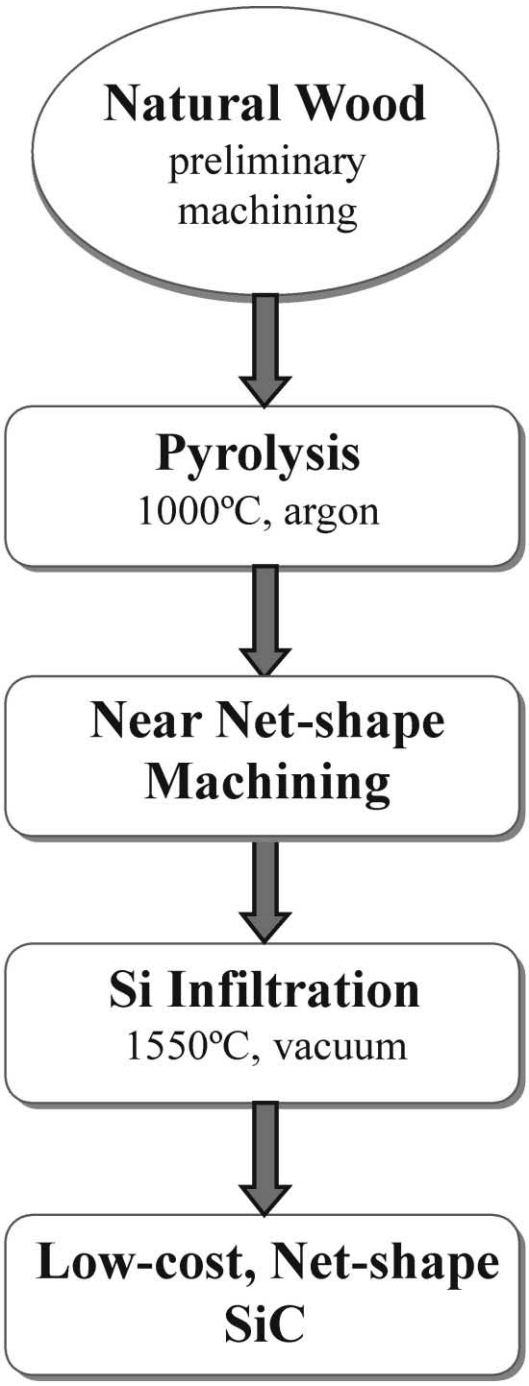

Fig. 1. Flow chart of the fabrication of biomorphic SiC.

2.2. Microstructural characterization

Microstructure of the carbon templates and of the undeformed and deformed SiC samples was studied by scanning electron microscopy (SEM) using an Philips XL30 microscope (Servicio de Microscopía Electrónica, Universidad de Sevilla), equipped with secondary electron (SE) and backscattered electron (BSE) detectors. Large porosity fractions in sections perpendicular to the axial growth direction were measured on SEM micrographs using a 100 point grid, both in the carbon templates and the infiltrated samples. As the microstructure presents a periodic structure, the points were randomly distributed, and the grid was rotated randomly after each measurement.

2.3. High-temperature deformation

Parallelepipeds, $3\times3\times5$ mm, were cut from the SiC materials (with the longer axis parallel to the axial direction). The specimens were tested in compression at 1150, 1250 and 1350 °C, in air, at constant cross-head speeds resulting in strain rates of 2×10^{-5} s^{-1}. The same conditions were used for tests run at 1150 and 1250 °C on samples cut with the longer axis perpendicular to the radial direction. Experiments were performed using an Instron screw-driven universal testing machine, model 1185, with a furnace mounted on its frame. Alumina rods with SiC pads were used. Load/time behavior was monitored on a chart recorder.

3. Results and discussion

3.1. Materials characterization

Final densities of the carbon templates were 0.34 ± 0.05 g cm^{-3} (white pine) and 0.33 ± 0.05 g cm^{-3} (Flanders pine), which is about 15% of the theoretical density of graphite (2.16 g cm^{-3}). Full reaction of such carbon densities with Si would result in aproximately 1.10 g cm^{-3}, which is approximately 34% of the theoretical density of SiC, in excellent agreement with our precursor selection criterium.

Fig. 2 shows the typical microstructure of the templates. Microstructure is similar for both types of pine, showing a combination of parallel open channels (average of 62 vol.% of the total section is large open porosity). Pine wood samples show unimodal cell size with cell size depending on the particular growth ring of the tree. In Fig. 2 we show the interfaces between consecutive rings both for white pine (Fig. 2a) and Flanders pine (Fig. 2b). The cells are nearly rectangular. The larger ones are about 20 μm in size, while the small ones are about 10 μm. Fig. 2c shows a section of the Flander pine carbon template parallel to the channels. As stated in the introduction, such microstructure is ideal for high temperature filters or catalyst carriers.

The infiltrated SiC materials have the microstructure shown in Fig. 3, basically isostructural to the carbon template (see Fig. 2 for comparison). The density of the final materials is 1.2 ± 0.1 g cm^{-3} for white pine and 1.7 ± 0.1 g cm^{-3} for Flanders pine. If all the carbon in the templates reacts, the maximum SiC density is about

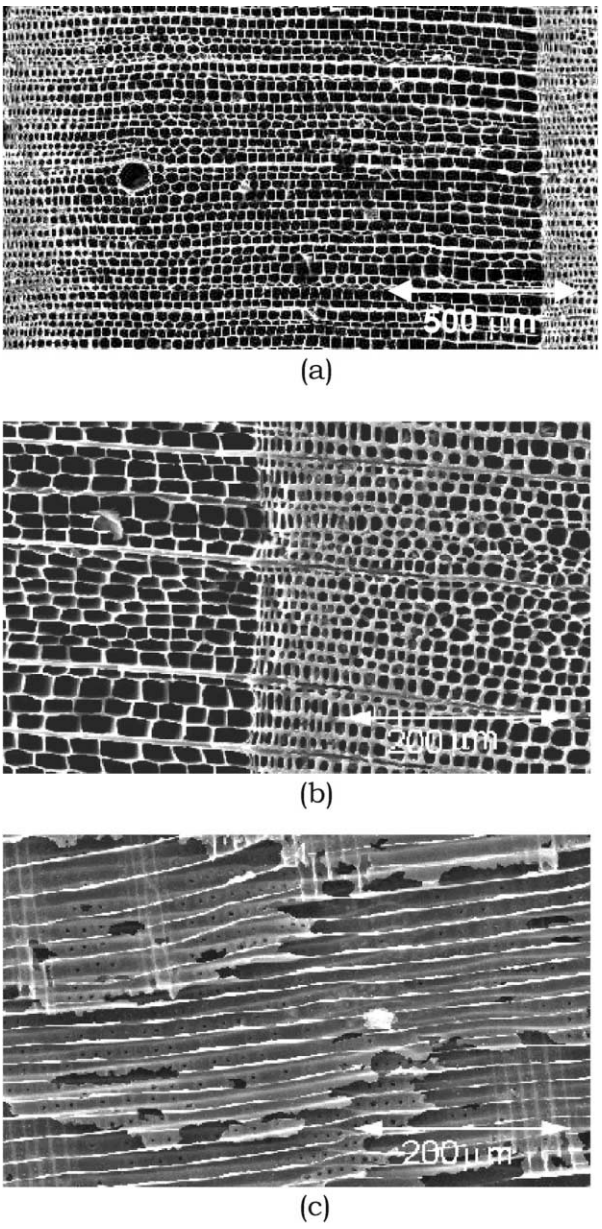

Fig. 2. SEM photomicrographs of carbon templates fabricated by pyrolysis. Sections perpendicular to axial direction of (a) white pine and (b) Flanders pine, and to (c) radial direction of white pine.

1.1 g cm^{-3} for both materials, so 0.1 and 0.6 g cm^{-3} of the final density is unreacted Si for white pine and for Flanders pine respectively.

The progress of the infiltration is documented in the SEM micrographs of Fig. 4, taken on partially infiltrated samples. The fibrous microstructure of the wood is reproduced in the SiC because the reaction is channeled by the porous wood microstructure. The connection between wood channels produces an interconnected SiC structure, thus allowing good mechanical properties despite the low density here.

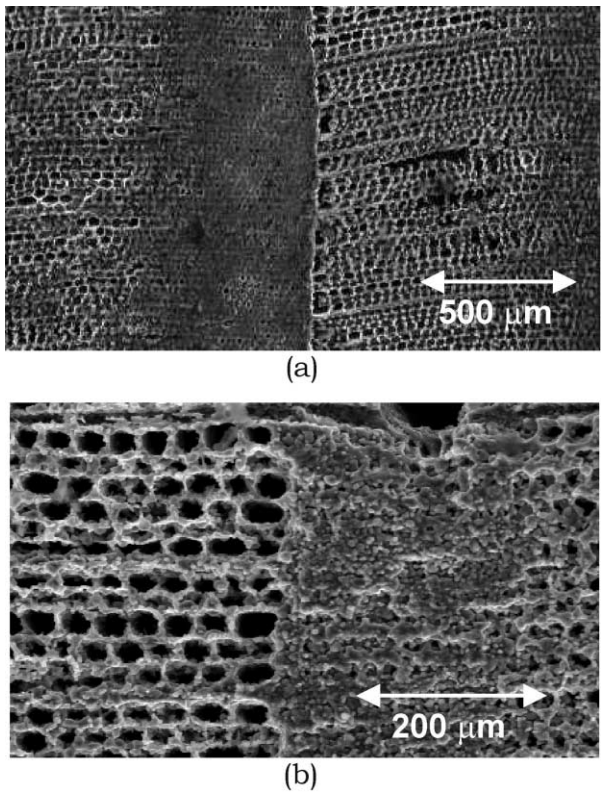

Fig. 3. SEM photomicrographs of the microstructure of as infiltrated pine-wood-based SiC. (a) White pine, showing season rings, and (b) Flanders pine.

3.2. Mechanical properties

Compressive strength experiments in the axial direction for both types of pine are summarized in Fig. 5. Tests were stopped when substantial weakening was observed. Samples did not exhibit catastrophic fracture. At 1150, 1250 and 1350 °C, the compressive strength for axial samples was respectively 69, 80 and 26 MPa for white-pine-based SiC and 204, 237 and 241 MPa for the Flanders-pine-based SiC.

In the radial direction results were 38.5 MPa at 1150 °C, and 13.3 MPa at 1250 °C for white pine and 7.2 MPa at 1250 °C for Flanders pine. These were the only reliable results. Numerous samples fractured upon loading during heating.

The weak correlation between temperature and compressive strength is evident. Given the low density of the samples, the interconnection of the SiC inside the fibrous structure may have reached a low point that critically controls mechanical properties. This may also explain the large difference between both types of pines, that have the same amount of SiC, and only differ in the amount of unreacted Si. It is possible that for low-density biomorphic SiC, the role that unreacted Si plays is more significant than for higher-density bimorphic SiC, probably by preventing early catastrophic fracture, and

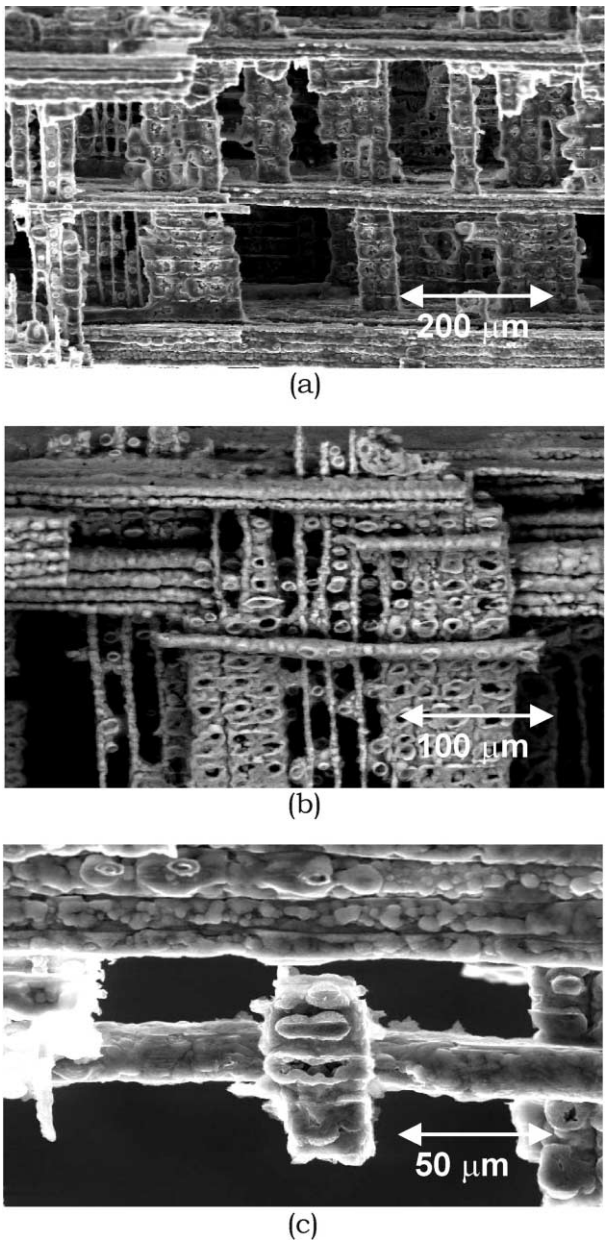

Fig. 4. SEM photomicrographs of the microstructure of partially infiltrated Flanders pine-wood-based SiC. (a) and (b) Details of the interconnected structure, (c) detail of the fibrous microstructure.

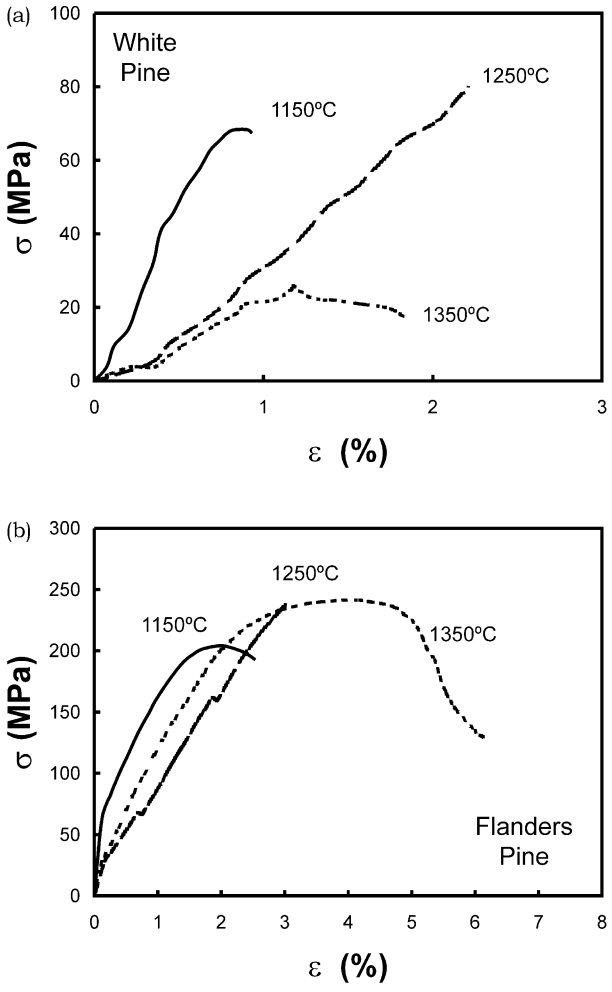

Fig. 5. Constant-compressive strain rate (2×10^{-5} s^{-1}) high-temperature deformation experiments on axial pine-wood-based SiC from (a) white pine, and (b) Flanders pine.

allowing a better response of SiC network. Considering white pine and Flanders pine good representatives of respectively very low and very high unreacted Si content, it is acceptable to average their mechanical response with a large error bar.

As mentioned above a good approach for the discussion of the mechanical properties of these materials is to consider that the strongly interconnected SiC microstructure is responsible of their behavior: the material can be regarded as a continuous network of SiC with residual Si. For relative densities below 30%, the model of Gibson and Ashby[4] proposes a potential dependence between the compressive strength (σ_c/σ_{ys}, where σ_c is the strength of the cellular solid and σ_{ys} is the strength of the fully dense material at a given temperature) and the relative density (ρ_c/ρ_s, where ρ_c is the cellular structure density and ρ_s is the full density), that varies with the type of microstructure and loading mode:

$$\frac{\sigma_c}{\sigma_{ys}} = C_1\left(\frac{\rho_c}{\rho_s}\right)^{\frac{3}{2}} \quad (2)$$

$$\frac{\sigma_c}{\sigma_{ys}} = C_2\left(\frac{\rho_c}{\rho_s}\right) \quad (3)$$

$$\frac{\sigma_c}{\sigma_{ys}} = C_3\left(\frac{\rho_c}{\rho_s}\right)^{2} \quad (4)$$

Eq. (2) describes foams in compression, Eq. (3) honeycombs in axial compression and Eq. (4) honeycombs in transverse compression. C_1, C_2, C_3, are experimental

constants. In the case of wood-derived SiC, in axial compression, it has been proposed that the crushing mechanism is a combination of the loading modes described by Eqs. (2) and (3), so values between 1 and 1.5 for the relative-density exponent are predicted. Honeycombs in transverse compression reproduce fairly well the mechanical conditions of the radial compression of SiC. For denser systems, higher order terms of the relative density are needed. However, a first approximation to the problem is qualitatively correct by these simple set of equations.

The values of the compressive strength of fully dense SiC have been taken from the literature:[25] 3600 MPa at 1150 °C, 2700 MPa at 1250 °C, 1800 MPa at 1350 °C. They correspond to a set of experiments run in a previous study, with the same machine, under identical experimental conditions and compression rates, on monolithic commercial SiC.

The average of relative values of the strength vs. the relative density of SiC are included in the plot presented in Fig. 6, that in addition to the results in this study shows the average of data taken from previous works on SiC based on different woods, in the intermediate range of densities.[11,19,20]

Porous reaction-formed SiC (RFSC) strengths have also been included in the plot. [25] The porous reaction formed SiC microstructure is isotropic, and resembles that of a foam. Data from these materials yield a relative density exponent of 3.4 ± 0.3 ($r^2=0.98$), higher than the proposed model, that predicts 1.5. It is interesting to note that the less anisotropic of the wood-based SiC, with a relative SiC density of approximately 60%, and derived from mango, is a good extrapolation of the non-anisotropic SiC data.

The relative density exponents for anisotropic biomorphic SiC under different load modes are also higher

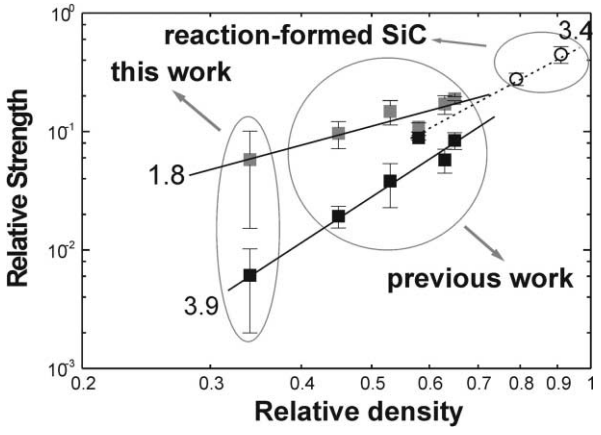

Fig. 6. Comparison of the average relative crashing strengths (see text for details) of pine-wood-based SiC with previous results on biomorphic SiC ceramics, and porous reaction-formed SiC. Slopes mark the behavior of isotropic (slope 3.4) anisotropic axial (slope 1.8) and radial (slope 3.9) samples.

that predicted: 1.8 ± 0.1 ($r^2=0.98$) in axial compression when 1–1.5 is predicted, and 3.9 ± 0.23 ($r^2=0.99$) in radial compression when 2 is predicted. The results obtained for the pine-wood derived SiC in this work confirm this relations between relative density and relative strength. Its behavior fits very well with the extrapolation for low densities of anisotropic biomorphic SiC data, both in the axial and radial direction. The microstructure of pine-wood derived SiC is consistent with these results, as it lacks long radial cells and the axial cells are very parallel. These two microstructural factors are critical to the level of anisotropy of strength.

The systematic shift might be related to the drastic simplifications assumed by taking only a first order approximation and to some scatter in the density and strength measurements. However, the values of the exponents increase in the correct way, with the relative density exponents of materials with isotropic response lying between those showing an anisotropic response when loaded axially and radially respectively, as predicted. The results on low-density pine-derived SiC obtained in this work support our previous interpretation of the mechanical behavior of biomorphic silicon carbide, and extend our understanding of these materials.

4. Conclusions

Low-density SiC has been fabricated by melt infiltration of pyrolized carbon templates from two types of pine. Wood precursors were selected using previous results for denser biomorphic SiC. The resulting porous microsctructure is anisotropic and highly interconnected. Partially infiltrated microstructures have allowed documentation of the infiltration process. The material has been tested for compressive strength at high temperature between 1150 and 1350 °C. The mechanical behavior shows high anisotropy. The normalized compressive strengths are a good extrapolation of previous studies with denser samples, and present a fair agreement with the model proposed by Gibson and Ashby for plastic collapse of cellular solids.

Acknowledgements

This work is supported by the Spanish Government, Ministerio de Ciencia y Tecnología, grant 1FD97–2335, and by the Andalusian Government under a "Ayuda para la Transferencia de Tecnología".

References

1. Wachtman, J. B., *Mechanical Properties of Ceramics*. John Wiley and Sons, New York, 1996.

2. Belitskus, D., *Fiber and Whisker Reinforced Ceramics for Structural Applications*. Marcel Dekker, New York, 1993.
3. Naslain, R., Materials design and processing of high-temperature matrix composites: state of the art and future trends. *Adv. Composite Mater*., 1999, **8**(1), 3–16.
4. Gibson, L. J. and Ashby, M. F. Cellular Solids: Structure and Properties. 1988, Pergamon Press.
5. Kovar, D., King, B. H., Trice, R. W. and Halloran, J. W., Fibrous monolithic ceramics. *J. Am. Ceram. Soc*., 1997, **80**(10), 2471–2487.
6. Alper, M., The Biological Membrane. *Mater. Res. Bull*, 1992, **17**, 53–60.
7. Mark, J. E. and Calvert, P. D., Biomimetic, hybrid and in-situ composites. *Mater. Sci. Eng*., 1994, **C1**, 159–170.
8. Greil, P., Lifka, T. and Kaindl, A., Biomorphic silicon carbide ceramics from wood: I and II. *J. Eur. Ceram. Soc*., 1998, **18**, 1961–1983.
9. Greil, P., Near net shape manufacturing of ceramics. *Mater. Chem. Phys*., 1999, **61**, 64–68.
10. Sieber, H., Hoffmann, C., Kaindl, A. and Greil, P., Biomorphic cellular ceramics. *Adv. Eng. Mater*., 2000, **2**(3), 105–109.
11. Martínez-Fernández, J., Varela-Feria, F. M. and Singh, M., Microstructure and thermomechanical characterizacion of bimorphic silicon carbide-based ceramics. *Scripta Mater*., 2000, **43**, 813–818.
12. Singh, M., Environment conscious ceramics (ecoceramics). *Ceram. Sci. Eng. Proc*., 2000, **21**(4), 39–44.
13. Martínez-Fernández, J., Varela-Feria, F. M., Domínguez Rodríguez, A. and Singh, M. Microstructure and thermomechanical characterization of biomophic silicon carbide-based ceramics. In *Environment Conscious Materials; Ecomaterials*. Canadian Institute of Mining, Metallurgy, and Petroleum, 2000, pp. 733–740.
14. Singh M. Environment conscious ceramics (ecoceramics): An Eco-friendly Route to Advanced Ceramic Materials. In *Proc. of 11th International Symposium on Ultra High Temperature Materials: High Temperature Materials Development for Global Environmental Protection*. Tajimi, Japan, 2001. NASA/CR-2001–211202, Glenn Research Center, Cleveland, OH, pp. 58–65.
15. Singh, M., *Environment Conscious Ceramics (Ecoceramics)*. NASA/TM 2001–210605, Glenn Research Center, Cleveland, Ohio, 2001.
16. Muñoz, A., Martínez-Fernández, J., Pinto Gómez, A. R. and Singh, M. Microstructure and high temperature compressive mechanical behavior of joints in biomorphic silicon carbide ceramics In *Joining of Advanced and Specialty Materials III*. ASM International, Materials Park, OH, USA, 2000, pp. 7–14.
17. Sieber, H., Kaindl, A., Schwarze, D., Werner, J. P. and Greil, P., Light-weight cellular ceramics from biological derived preforms. *Ceram. Forum Int., CFI/Ber. DKG 77*, 2000, **1–2**, 21–24.
18. Sieber, H., Kaindl, A., Friedrich, H. and Greil, P., Crystallization of SiC on biological carbon precursors. In *Ceram. Trans*., Vol., **110**, (*Bioceramics: Materials and Applications III*), ed. L. George, R. P. Rusin, G. S. Fischman, and V. Janas. The American Ceramic Society, 2000 81–92.
19. Varela-Feria, F. M., López Pombero, S., Martínez-Fernández, J., de Arellano López, A. R. and Singh, M., Creep resistant biomorphic silicon-carbide based ceramics. *Ceram. Eng. Sci. Proc*., 2001, **22**(3), 135–145.
20. Varela-Feria, F. M., López Pombero, S., de Arellano López, A. R. and Martínez-Fernández, J. Maderas cerámicas: fabricación y propiedades del carburo de silicio biomórfico. *Bol. Soc. Esp. Ceram. y Vidrio*, 2002 (in press).
21. Singh, M. and Behrendt, D. R., Reactive melt infiltration of silicon-niobium alloys in microporous carbon. *J. Mater. Res*., 1994, **9**, 1701–1705.
22. Varela Feria, F. M. Fabricación caracterización microestructural del carburo de silico biomórfico. Master thesis, Universidad de Sevilla, 2001.
23. López-Pombero, S. Comportamiento mecánico a alta temperatura de SiC biomórfico. Master thesis, Universidad de Sevilla, 2001.
24. Varela-Feria, F. M., López Pombero, S., Martínez-Fernández. J., de Arellano López, A. R. and Singh, M. Precursor selection for property optimization in biomorphic SiC ceramics. *Ceram. Eng. Sci. Proc*., 2002 (in press).
25. Muñoz, A., Martínez Fernández, J., Domínguez Rodríguez, A. and Singh, M., High temperature compressive strength of reaction formed silicon carbide (RFSC) ceramics. *J. Eur. Ceram. Soc*., 1998, **18**, 65–68.